Brain Somatostatin Receptors Are Up-Regulated In Somatostatin-Deficient Mice

Article *in* Molecular Endocrinology · September 2002

Impact Factor: 4.02 · DOI: 10.1210/me.2002-0068 · Source: PubMed

7 authors, including:

Marcelo Rubinstein

CONICET - National Scientific and Technical …

131 PUBLICATIONS **7,937** CITATIONS

SEE PROFILE

0888-8809/02/$15.00/0
Printed in U.S.A.

Molecular Endocrinology 16(8):1951–1963

doi: 10.1210/me.2002-0068

Brain Somatostatin Receptors Are Up-Regulated In Somatostatin-Deficient Mice

JOSÉ L. RAMÍREZ, RANIA MOUCHANTAF, UJENDRA KUMAR, VERONICA OTERO CORCHON, MARCELO RUBINSTEIN*, MALCOLM J. LOW, AND YOGESH C. PATEL

Fraser Laboratories (J.L.R., R.M., U.K., Y.C.P.), Departments of Medicine, Pharmacology and Therapeutics, Neurology and Neurosurgery, McGill University and Royal Victoria Hospital, Montréal, Québec, Canada, H3A 1A1; and The Vollum Institute (V.O.C., M.R., M.J.L.), Oregon Health & Science University, Portland, Oregon 97201

The peptide somatostatin (SST) is widely synthesized in the brain and periphery and acts through a family of five receptors (SSTR1-5) to exert numerous effects. A gene product related to SST, cortistatin (CST), also interacts with SSTR1-5. Here we have investigated the regulation of SSTR1-5 and of CST in SST knockout (SSTKO) mice. The five SSTRs were quantitated individually by subtype-selective binding analysis, by immunocytochemistry, and by mRNA measurement and showed, in the brain of SSTKO mice, up-regulation of subtypes 1, 2, 4, and 5, and down-regulation of SSTR3. Peripheral tissues displayed both subtype- and tissue-specific changes in SSTR1-5 mRNA levels of expression. Lack of SST did not up-regulate normal CST expression in brain nor did it induce its expression in the periphery. SST-like immunoreactivity, however, was induced in the proximal midgut in SSTKO animals, suggesting intestinal expression of a novel SST-like gene. (*Molecular Endocrinology* 16: 1951–1963, 2002)

SOMATOSTATIN (SST), A REGULATORY peptide with two bioactive forms, SST-14 and SST-28, is produced in neuroendocrine cells in the brain and periphery and acts on a wide array of tissue targets to modulate neurotransmission, cell secretion, and cell proliferation (1–3). Marked changes in brain and cerebrospinal fluid levels of SST occur in several neurodegenerative diseases including Alzheimer's and Huntington's disease and AIDS encephalopathy (4–8). The actions of SST are mediated by a family of G protein-coupled receptors (GPCRs) with five subtypes (SSTR1-5) encoded by separate genes (3, 9). The five SSTRs are variably expressed in brain. In the rat, mRNA for SSTR1 is the most abundant followed by SSTR2, SSTR5, SSTR3, and SSTR4 (3, 10–13). A high density of neurons positive for SSTR1 and SSTR2 and moderate density of SSTR5-expressing neurons occur in the deeper layers of the cerebral cortex (14, 15). SSTR3 localizes mainly in the cerebellum (3). All five SSTRs are also expressed in the pituitary, islets, gut, and aorta (16–18). SSTRs are extensively regulated at the membrane by agonists (19). SSTR2, 3, 4, and 5 undergo rapid agonist-dependent endocytosis. SSTR1 does not internalize but is instead up-regulated in response to continued agonist treatment (19, 20).

Recently, a second SST-related gene, cortistatin (CST), has been identified in humans and rodents which gives rise to two cleavage products comparable to SST-14 and SST-28, CST-14 and CST-29 in the rat and CST-17 and CST-29 in humans, but only a putative CST-14 in the mouse (21–24). Unlike the broad distribution of SST, expression of CST is restricted to interneurons in the cerebral cortex and hippocampus. CST-14 shares 11 of 14 amino acid residues with SST-14 and binds to the five SSTRs with high affinity. The actions of CST overlap with those of SST but also include additional novel effects on sleep, suggesting that CST has independent biological functions (21).

We have investigated the effect of SST deficiency on the regulation of SSTR1-5 expression and of the CST gene in SST gene knockout (SSTKO, SST −/−) mice. These mice are born normally and grow to adulthood with no obvious physiological or anatomical defect of the brain or peripheral organs (25). They display neuroendocrine abnormalities in GH secretion and mildly increased seizure severity (26), but it is not known whether the CST gene compensates for SST deficiency (25). We have compared the pattern of expression of SSTR1-5, SST, and CST expression in different brain regions and in peripheral tissues of control and SSTKO mice. We show that loss of endogenous SST induces subtype-specific alterations in SSTR expression with a net increase in brain membrane SSTRs. SST deficiency did not alter brain CST levels nor did it induce *de novo* expression of the CST gene in the periphery. It was, however, associated with the expression of a novel, hitherto unknown, SST-like species in the upper intestine and pancreas.

Abbreviations: CST, Cortistatin; CST-LI, CST-like immunoreactivity; GPCR, G protein-coupled receptor; hSSTR, human SSTR; [^{125}I]-LTT STT-28, ^{125}I-labeled Leu^{8}-DTrp^{22}-Tyr^{25}, SST-28; SST, somatostatin; SSTKO, SST knockout; SST-LI, SST-like immunoreactivity; SSTR, SSR receptor; wt, wild-type.

RESULTS

Quantitation of Individual SSTR Subtypes by Binding Analysis

The total population of SSTRs in brain of control and SSTKO mice was analyzed by saturation binding analysis of membranes isolated from whole brain using as radioligand [^{125}I]-labeled Leu^{8}-D-Trp^{22}-Tyr^{25}, SST-28 ([^{125}I]-LTT SST-28), which binds to all five SSTRs with comparable affinity. In addition, saturation binding analysis with [^{125}I]-LTT SST-28 in the presence of an excess of subtype-selective nonpeptide analogs permitted a quantitative analysis of the membrane concentration of each individual SSTR subtype as a component of the total receptor population. Figure 1 depicts saturation isotherms of specific [^{125}I]-LTT SST-28 binding to membranes from whole brain of wild-type (wt) and SSTKO animals in the presence of excess SST-14 or nonpeptide SST analogs. Scatchard analysis of maximal binding (B_{max}) and dissociation constant (K_d) values obtained from these binding data are shown in Table 1. There was a net increase in the level of expression of total [^{125}I]-LTT SST-28 binding sites in SSTKO mice (Fig. 1, panel A). Scatchard analysis revealed a 116% increase in binding capacity (B_{max}) in SSTKO mice compared with control, from 147 $\pm$ 4.4 to 317 $\pm$ 29 fmol/mg protein ($P < 0.001$) without any change in ligand binding affinity (K_d) (Table 1). Separate analysis of the individual SSTR subtypes revealed a significant increase in B_{max} of SSTR1 (103%), SSTR2 (106%), SSTR4 (38%), and SSTR5 (110%) in the SSTKO mouse brains (Fig. 1 and Table 1). In contrast, the level of SSTR3 selective binding sites was reduced by 38% in the SST-deficient animals. There was no significant change in ligand binding affinity (K_d) for any of the SSTR subtypes in the control and KO animals.

Expression of SSTR1-5 mRNA in Brain

The mean levels of mRNA for each receptor quantified from Southern hybridization of RT-PCR signals by densitometry are shown in Fig. 2. All five SSTR mRNAs were detected in normal mouse brain with the following relative abundance: SSTR1 = SSTR2 > SSTR3 > SSTR4 = SSTR5. mRNA for SSTR1, SSTR2, and SSTR5 displayed significant 201%, 178%, and 163% increases in the SST-deficient mice compared with control. On the other hand, SSTR3 mRNA showed a significant 57% decrease in the level of expression whereas SSTR4 mRNA was unchanged.

The results of SSTR1-5 mRNA expression in different brain regions analyzed by semiquantitative RT-PCR are presented in Fig. 3. In both the wild-type (wt) and knockout mice, expression of all five SSTRs was detectable in most brain regions tested. As in the case of whole brain, SSTR1 mRNA displayed significant up-regulation in most brain regions including the cerebral cortex, thalamus, cerebellum, midbrain, brainstem, and spinal cord (Fig. 3A). Striatal SSTR1 mRNA, however, was unchanged whereas SSTR1 mRNA expression in the hypothalamus was dramatically reduced in the SST-deficient mice. Like SSTR1 mRNA, SSTR2 mRNA was also significantly increased in several prominent central nervous system regions including the cerebral cortex, striatum, hypothalamus, and spinal cord but was unchanged in the thalamus, cerebellum, midbrain, and brainstem (Fig. 3B). SSTR3 mRNA was down-regulated in the olfactory bulb, cerebral cortex, striatum, and midbrain without significant changes in other brain regions (Fig. 3C). SSTR5 mRNA showed significant increases in frontal cortex, hypothalamus, and midbrain (Fig. 3E). Regional brain expression of SSTR4 mRNA was unaltered in the SSTKO mice except for a significant increase in the brainstem (Fig. 3D).

Expression of SSTR1-5 Protein in Brain by Immunocytochemistry

The pattern of expression of SSTR1-5 protein in the brain of the SST-deficient mice was analyzed directly by immunocytochemistry and represented in coronal sections through the frontal cortex of control and SSTKO mice (Fig. 4). SSTR1-5 immunoreactivity was localized as a dark brown reaction product by peroxidase immunocytochemistry and expressed both as a membrane and cytoplasmic protein (Fig. 4, A–J). In wt mice, SSTR1-like immunoreactivity was observed in pyramidal neurons in layer 5 and in interneurons in layer 2. Positively labeled cells also exhibited strong staining of dendrites and processes extending through the neuronal somata. SSTKO mice displayed a 28% increase in the number of SSTR1-positive neurons as well as denser staining of the labeled neurons (Fig. 4, A, B, and K). SSTR2-positive neurons were sparsely distributed throughout the cortical layers mainly in interneurons and in occasional pyramidal cells; they lacked any clear laminar distribution (Fig. 4, C and D). In the SSTKO mice, SSTR2 immunoreactivity was more intense in layer 2 and in the deeper layers, especially layer 5 where it showed a clear laminar distribution. Immunostaining was associated with neuronal perikarya as well as with neuronal processes and dendrites (Fig. 4). Quantitative analysis revealed a 23% increase in the number of SSTR2-positive neurons in the SSTKO mice (Fig. 4). SSTR3 immunoreactivity in control mice was strongly expressed throughout the cortex in both pyramidal and nonpyramidal neurons, being concentrated in nerve cell bodies in the upper layers (2 and 4) and in both cell bodies and processes in the deeper layers (5 and 6) (Fig. 4E). In the SSTKO mice, there was a 33% reduction in the number of SSTR3-immunostained neurons, and the labeling was less intense in all the positively labeled structures (Fig. 4, F and K). SSTR4-like immunoreactivity was moderately well expressed in neurons and cell processes throughout the cortex with no difference in the level of expression between wt and SSTKO mice (Fig.

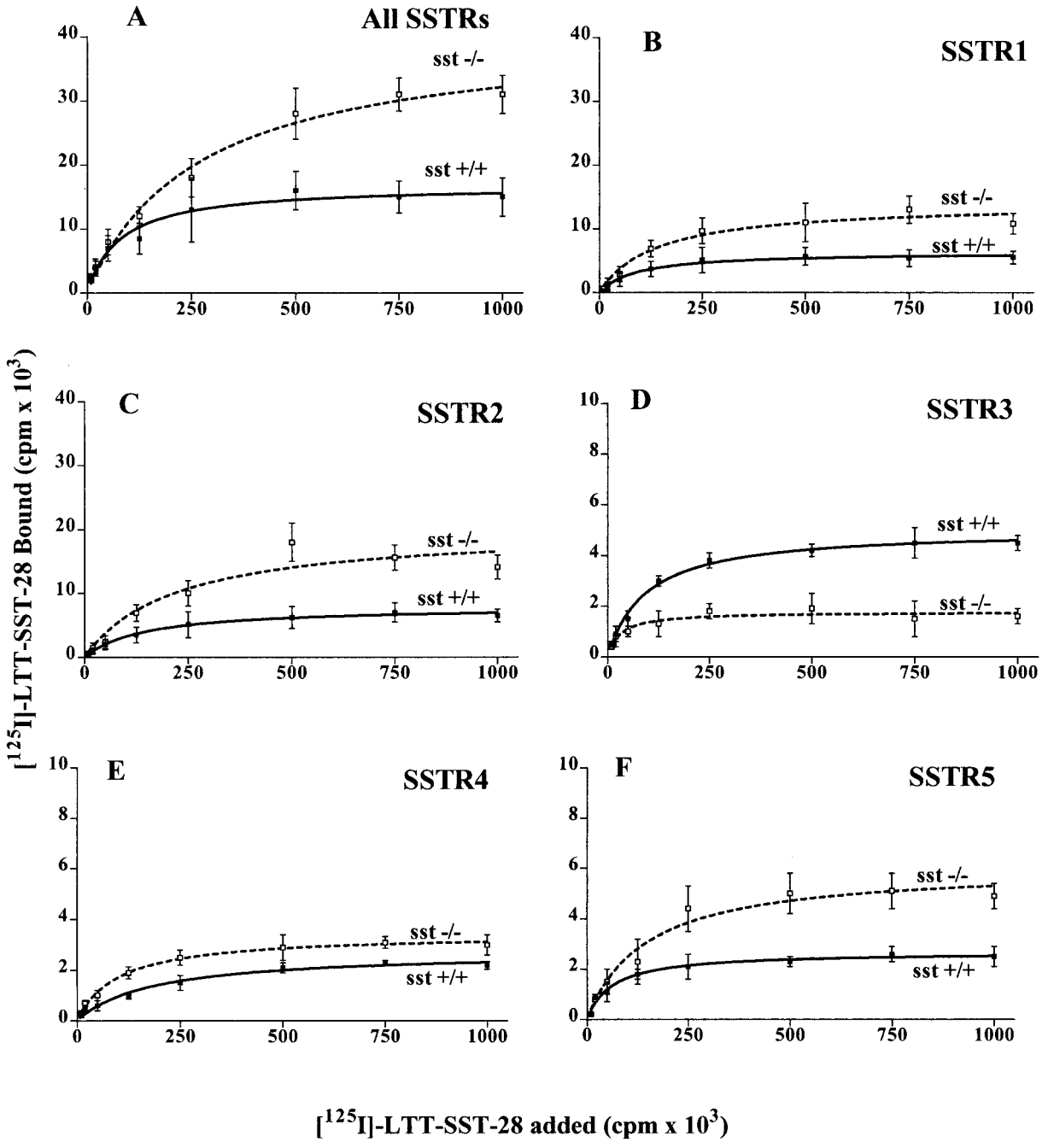

Fig. 1. Saturation Isotherms of [^{125}I]-LTT-SST-28 Binding to Membranes Prepared from Whole Brain

Membranes were incubated with increasing concentrations of radioligand and assayed for binding in the absence or presence of 100 nM SST-14 (to quantitate the total population of SSTRs, panel A) or 100 nM or 1 μM of subtype monospecific nonpeptidic SSTR analogs (to quantitate individual SSTR subtypes, panels B–F). wt (sst +/+, *solid lines*), SSTKO (sst −/−, *dotted lines*). Data represent the mean of at least three separate membrane preparations from different animals, performed in wt and SSTKO brain pairs.

4, G and H). SSTR5 was the least expressed subtype in control cortex with relatively selective expression both in perikarya and in dendrites in neurons confined to layer 5 (Fig. 4I). SSTKO mice displayed increased SSTR5 expression in layers 5 and, to a lesser extent, in layer 2 (Fig. 4J). There was an 18–20% increase in the number of SSTR5 (Fig. 4J)-labeled neurons (Fig. 4K).

Expression of SSTR1-5 mRNA in Peripheral Tissues

Because of the known high level expression of SSTRs in human and rat peripheral tissues such as the pituitary, islet cells, gastrointestinal tract, adrenals, and gonads, these organs were selected for SSTR analy-

Table 1. Binding Analysis of Total SSTRs and Individual Subtypes in Whole Brain Membranes from wt (sst +/+) and SSTKO (sst −/−)

	sst +/+		sst −/−	
	B_{max} (fmol/mg protein)	K_d (nM)	B_{max} (fmol/mg protein)	K_d (nM)
All SSTRs	147 ± 4.4	0.86 ± 0.2	317 ± 29[a]	0.69 ± 0.24
SSTR1	59 ± 2.6	0.91 ± 0.39	120 ± 4.6[a]	0.92 ± 0.14
SSTR2	64 ± 8	0.84 ± 0.15	133 ± 26[b]	1.08 ± 0.2
SSTR3	43 ± 11	1.17 ± 0.26	17 ± 2.2[c]	0.81 ± 0.1
SSTR4	16.9 ± 0.88	0.61 ± 0.14	23 ± 1.4[c]	0.62 ± 0.14
SSTR5	23.3 ± 0.95	0.27 ± 0.05	49 ± 3.7[b]	0.4 ± 0.17

n = 3; see Fig. 1 legend for details.
[a] $P < 0.001$ *vs.* wt.
[b] $P < 0.01$.
[c] $P < 0.05$.

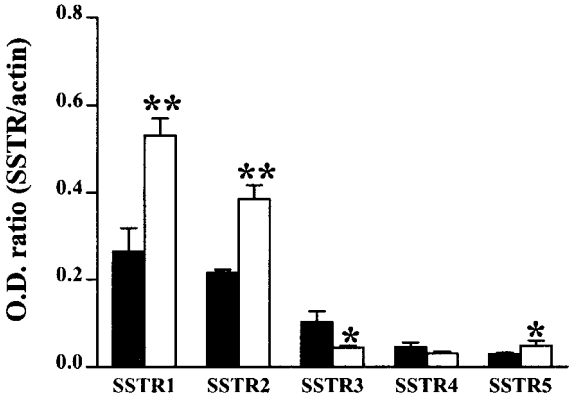

Fig. 2. SSTR1-5 mRNA Expression in Whole Brain

SSTR mRNA was quantitated from Southern hybridization signal of RT-PCR products of wt (*solid columns*) and SSTKO (*open columns*) mice. Densitometric analysis was performed using the software Vista Scan 2.4 and the total intensity (average optical density × area in pixels) was quantified with the Igor Pro 3.13 analysis software package. The arbitrary units were collected for background and expressed as a ratio of actin mRNA. Data are expressed as mean ± SE of four measurements of optical densities of hybridization signals from three separate experiments. *, $P < 0.05$; **, $P < 0.02$; *vs.* corresponding wt.

sis. In addition, the liver was included as a SSTR-poor tissue for comparison (Fig. 3). In control mice, SSTR1 mRNA was abundantly expressed in the pituitary, displayed moderate levels in the pancreas, stomach, and adrenals, but was absent in the liver and gonads (Fig. 3). In the SSTKO mice, SSTR1 expression was up-regulated only in the stomach but not in the other receptor-positive tissues; in the adrenals, mRNA for SSTR1 was significantly decreased. In the case of SSTR2 mRNA, control mice displayed high-level expression of this subtype in adrenals and pancreas, moderate levels in the pituitary and gonads, and no expression in the stomach and liver (Fig. 3B). As in the brain, the pancreas in the SSTKO mice showed significant up-regulation of this receptor subtype, but unlike the brain, the pituitary and adrenals displayed 40–50% reduction in mRNA. SSTR3 mRNA was normally detectable in the pituitary, pancreas, and gonads and showed a significant decrease in the SSTKO mice only in the pancreas with no change in the other organs (Fig. 3C). SSTR4 mRNA was present in high concentrations in the pancreas and in low amounts in the pituitary but was absent in all other peripheral tissues tested (Fig. 3D). Pancreatic expression of this subtype mRNA showed a small but significant reduction in the SSTKO mice. Among the peripheral tissues, SSTR5 mRNA was identified in the pancreas, pituitary, and gonads and exhibited a significant increase in the pituitary and a reduction in the pancreas in the SSTKO mice (Fig. 3E).

Expression of CST mRNA in Brain and Peripheral Tissues

Expression of CST mRNA was determined in whole brain, brain regions, and peripheral tissues of control and SSTKO mice and was compared with SST mRNA simultaneously measured in the same tissues. As expected, SST mRNA was undetectable in the SSTKO mice. CST mRNA expression in whole brain of the knockout mice was similar to that in controls. Analysis of SST mRNA in different brain regions showed detectable levels in all brain areas of control mice with the highest concentration in the frontal cortex (Fig. 5A). CST mRNA in control mice was also detectable in most brain regions tested (Fig. 5B), which included the olfactory bulb, cerebral cortex, striatum, thalamus, hypothalamus, and midbrain. It was absent, however, in the cerebellum, brainstem, and spinal cord. As in whole brain, there was no significant difference in the level of CST mRNA expression in different brain regions of the SST KO mice compared with controls.

In peripheral tissues, SST mRNA was readily detected in the pancreas, stomach, and pituitary of control mice but not in the liver, gonads, or adrenal glands (Fig. 5A). None of the peripheral tissues of the control

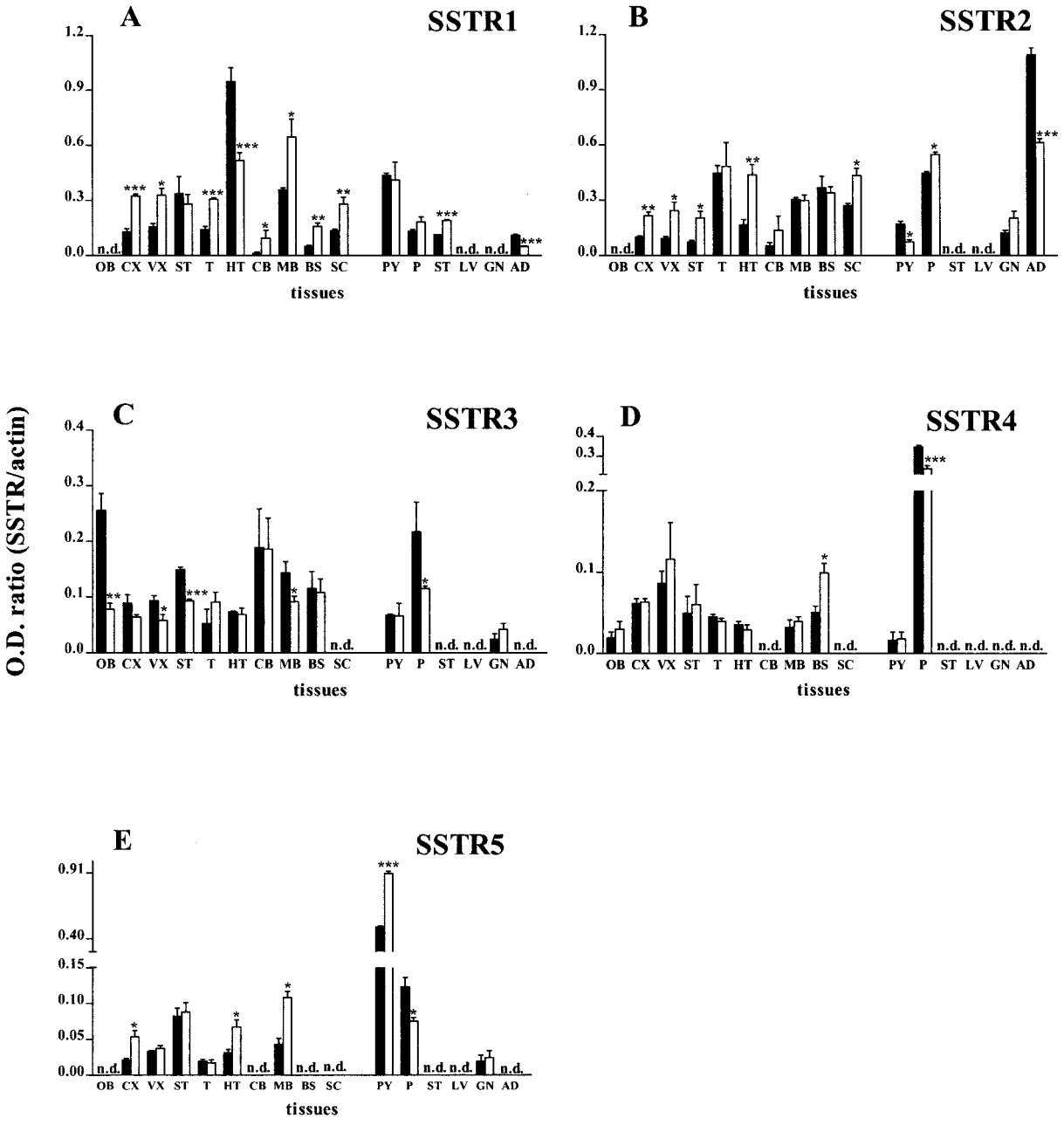

Fig. 3. SSTR1-5 mRNA Expression in Central Nervous System Regions and in Peripheral Tissues

SSTR1 (panel A), SSTR2 (panel B), SSTR3 (panel C), SSTR4 (panel D), and SSTR5 (panel E) mRNA expression was analyzed by semiquantitative RT-PCR in different brain regions and in peripheral tissues from wt (*solid columns*) and SSTKO (*open columns*) mice. See Fig. 2 for further details of mRNA analysis and quantification. OB, Olfactory bulbs; CX, frontal cortex; VX, visual cortex; ST, striatum; T, thalamus; HT, hypothalamus; CB, cerebellum; MB, midbrain; BS, brain stem; SC, spinal cord; PY, pituitary; P, pancreas, ST, stomach; LV, liver; GN, gonads; AD, adrenals. *, $P < 0.05$; **, $P < 0.02$; ***, $P < 0.001$ *vs*. corresponding wt. n = 3; n.d., nondetectable.

or SSTKO mice displayed any expression of CST mRNA (Fig. 5B).

Expression of SST and CST Immunoreactive Proteins

Whole-brain extracts of control mice contained 4.4 ± 0.63 ng SST-like immunoreactivity (SST-LI)/mg total protein. Because the RIA used for measuring SST-LI detects both SST and CST immunoreactivities, the total material represented a mixture of both SST- and CST-like peptides. Deletion of the SST gene resulted in a 95% reduction in total brain SST-LI in the SST-KO mice to a level of 0.197 ± 0.01 ng/mg protein. The small residual immunoreactivity of approximately 5%

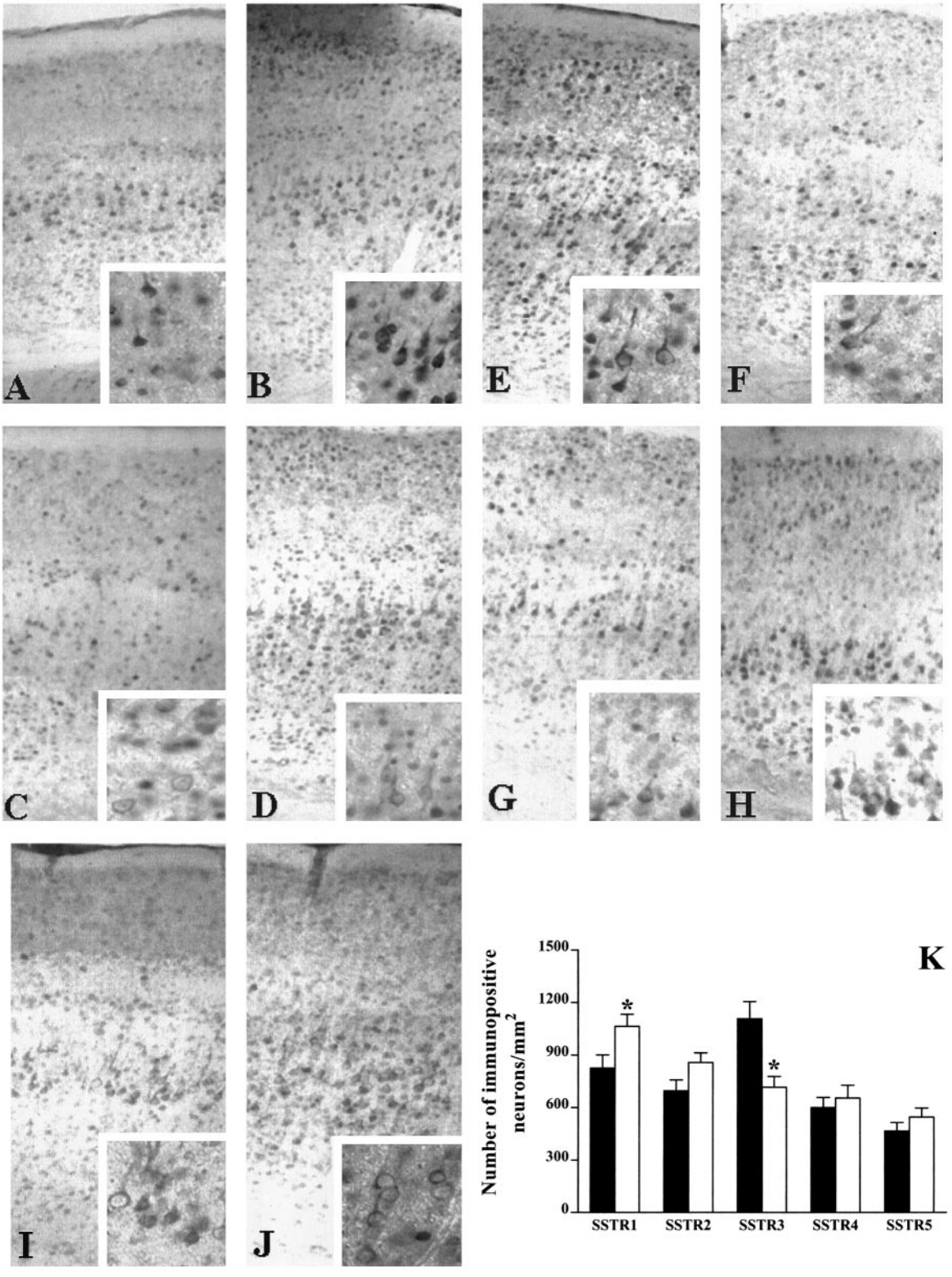

Fig. 4. Photomicrographs Illustrating Immunohistochemical Localization of SSTR1-5 in Brain Cortex

SSTRs were visualized in cortex of both wt (sst +/+, *left-hand panels*) and SSTKO mice (sst −/−, *right-hand panels*) as a *brown* reaction product by peroxidase immunocytochemistry, using SSTR1-5 subtype-specific rabbit antibodies. *Scale bar*, 25 μm. The *insets* show high-power views of selected SSTR-positive neurons illustrating receptor localization in membranes of cell bodies and diffusely in cytoplasm of neuronal processes. Lower magnification, ×100; *inset* magnification, ×400. Panels A and B, SSTR1; panels C and D, SSTR2; panels E and F, SSTR3; panels G and H, SSTR4; panels I and J, SSTR5. Panel K depicts the number of immunopositive neurons per mm^2 for each SSTR subtype. Mean ± SE. *, $P < 0.05$ *vs*. corresponding wt. n = 3.

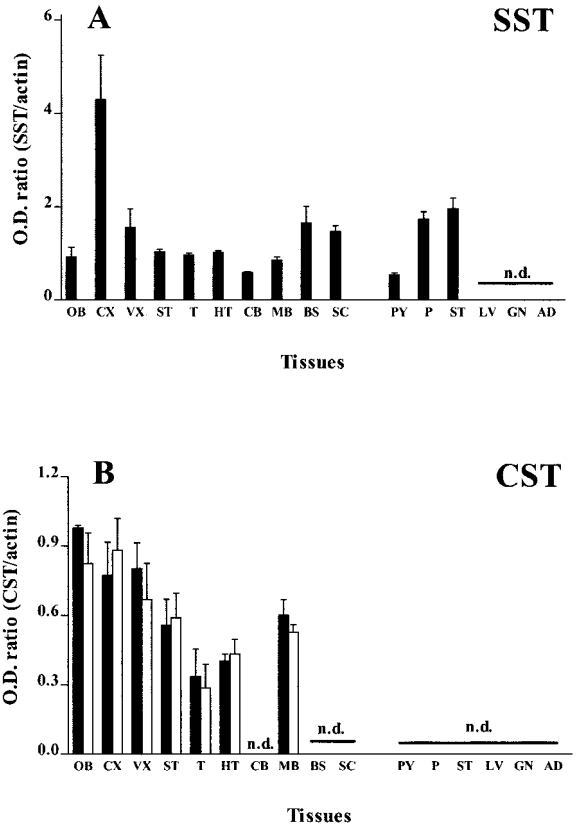

Fig. 5. SST and CST mRNA Expression in Different Brain Regions and in Peripheral Tissues

SST (panel A) and CST (panel B) mRNA expression was analyzed by semiquantitative RT-PCR in different brain regions and in peripheral tissues from wt (*solid columns*) and SSTKO (*open columns*) mice. OB, Olfactory bulbs; CX, frontal cortex; VX, visual cortex; ST, striatum; T, thalamus; HT, hypothalamus; CB, cerebellum; MB, midbrain; BS, brain stem; SC, spinal cord; PY, pituitary; P, pancreas, ST, stomach; LV, liver; GN, gonads; AD, adrenals. Mean ± SE. n = 3. n.d., Nondetectable.

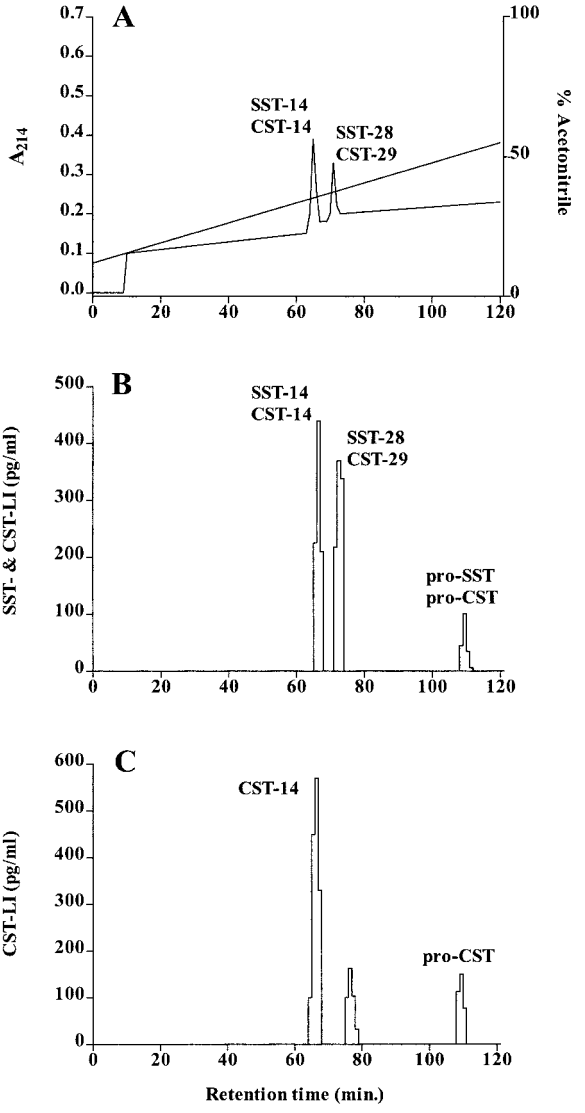

Fig. 6. HPLC Profiles of SST/CST-LI in Brain Extracts

Panel A illustrates the elution position of synthetic rat SST-14/CST-14 (retention time, 67 min) and SST-28/CST-29 (retention time, 73 min) standards detected by absorbance at 214 nm. Synthetic SST-14 and SST-28 coelute with CST-14 and CST-29, respectively. Panels B and C represent control and SSTKO mice samples, respectively. Profiles are representative of four separate extraction experiments from different animals.

in the SST-KO mice suggests a ratio of 19:1 for SST: CST-like peptides in mouse brain. To characterize the nature of endogenous CST peptides present in brain, whole-brain extracts from both control and SSTKO mice were fractionated by HPLC and the eluant was analyzed by RIA. The elution positions of the peaks obtained were compared with those of synthetic SST-14, CST-14, SST-28, and CST-29 under identical conditions. As shown in Fig. 6A, synthetic SST-14 coeluted with CST-14 (retention time, 67 min), and likewise synthetic SST-28 coeluted with CST-29 (retention time, 73 min). Thus, under the conditions of HPLC analysis that were used, the CST and SST peptides in the same sample were indistinguishable. The HPLC profile of whole-brain extracts from control animals (Fig. 6B, representative profile of four separate extractions) showed two major peaks corresponding to SST-14/CST-14 (46% of total immunoreactivity) and SST-28/CST-29 (34% of total immunoreactivity), respectively. A third peak of retention time, 110 min, accounted for 20% of the total immunoreactivity and corresponded to higher molecular weight precursor forms of both peptides (pro-SST and pro-CST). HPLC analysis of brain extracts of SSTKO mice revealed three peaks corresponding to CST-14 (66% of total immunoreactivity), a novel peak eluting after synthetic CST-29 at 77 min (18% of total immunoreactivity), and a peak at 110 min corresponding to pro-CST (16% of total immunoreactivity) (Fig. 6C).

Although the peripheral tissues of the SSTKO mice were negative for CST mRNA expression, analysis of

SST-LI by RIA revealed measurable quantities of immunoreactivity in pancreas, duodenum, jejunum, and ileum (Fig. 7). Indeed, the duodenal and jejunal concentrations of SST-LI in the SSTKO mice were comparable to the levels in control mice. To characterize this immunoreactivity further, duodenal extracts from wt and SSTKO mice were fractionated by HPLC (Fig. 8). Compared with wt duodenum, which expressed a single peak of retention time of 67 min corresponding to SST-14 (panel A), the SSTKO mouse duodenum featured two peaks, a minor peak with retention time of 67 min and a major peak that eluted at 115 min, 5 min after the elution position of pro-SST/pro-CST (panel B). Because this material could not be derived from either the SST or the CST gene, it appears to be the product of an unknown third SST-related gene expressed at high levels in the midgut.

DISCUSSION

The present study is the first comprehensive report of the *in vivo* regulation of SSTRs in the absence of their principal natural ligand SST. As in the rat, SSTR1 and SSTR2 were the predominant subtypes. SSTR3 mRNA was expressed throughout the mouse brain, in agreement with Fehlmann *et al.* (27). Moreover, in the mouse cerebellum, we found expression of not only SSTR3, the sole isoform described in the rat (12, 28), but also SSTR1 and SSTR2. SSTR5, which is moderately well expressed in the rat brain (13), was the least well expressed subtype in the mouse brain, in accordance with previously reported studies (27, 29). Such prominent differences in the pattern of SSTR expression between rat and mouse, two closely related species, suggest that there is no fixed pattern of expression of these receptors, because they are likely regulated dynamically in a subtype-, tissue-, and species-specific manner.

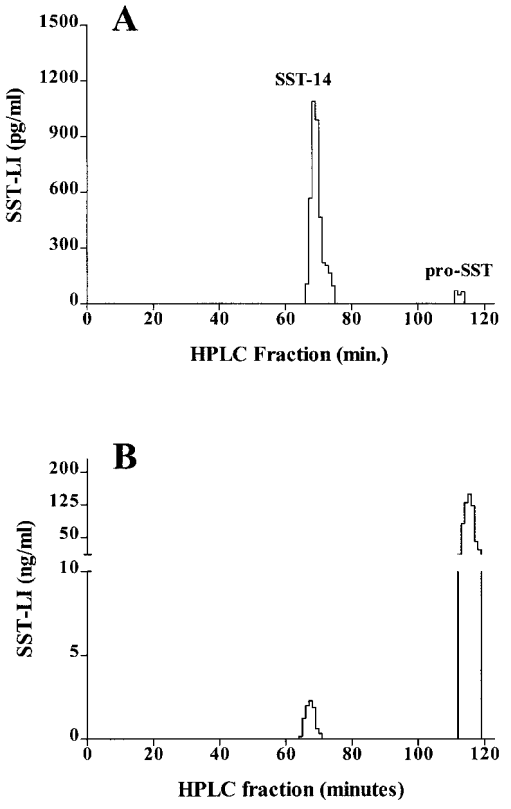

Fig. 8. HPLC Profiles of SST-LI in Duodenal Extracts

See Fig. 6 for details of HPLC analysis. Panel A, Control mice; panel B, SSTKO mice. Profile is representative of three experiments.

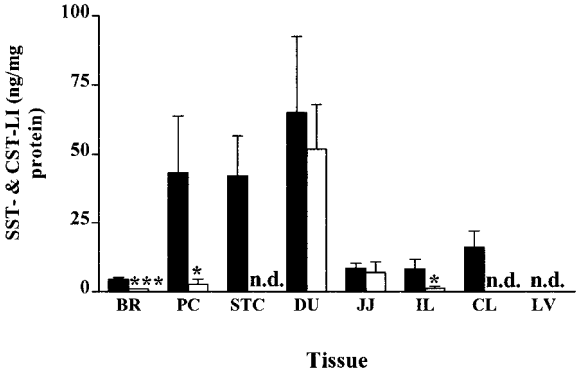

Fig. 7. SST/CST-LI in Whole Brain and Peripheral Tissues from Control (*solid columns*) and SSTKO (*open columns*) Mice

Results are expressed as nanograms of immunoreactive protein per milligram total protein. Brains from sst −/− mice contain small but readily detectable quantities of immunoreactivity representing 4.46 ± 0.53% of total immunoreactivity, presumably representing immunoreactive CST. Detectable SST/CST-LI are shown in pancreas, duodenum, jejunum, and ileum of SSTKO animals. BR, Whole brain; PC, pancreas; STC, stomach; DU, duodenum; JJ, jejunum; IL, ileum; CL, colon; LV, liver; n.d., nondetectable concentration. Values are mean ± SE of nine experiments. *, $P = 0.05$; **, $P < 0.01$ *vs*. wt.

In the present study, we analyzed both the total population of membrane SSTRs as well as the five individual SSTR subtypes by three independent techniques, saturation binding in the presence of subtype monospecific analogs, immunocytochemistry using subtype-selective antibodies, and mRNA analysis by semiquantitative RT-PCR. SST deficiency induced a 116% increase in total brain membrane SSTRs measured by binding analysis with a nonselective radioligand that binds to all five SSTR subtypes. Characterization of the individual subtypes by binding analysis showed a doubling of the level of expression of SSTR1, 2, and 5 associated with a 38% reduction in the level of SSTR3 binding sites and a comparable increase in SSTR4 binding sites. These findings were correlated by quantitative immunohistochemical analysis of SSTR-immunopositive neurons in the cerebral cortex and revealed an increase in the number of neurons expressing SSTR1, 2, and 5 together with a

decrease in SSTR3-positive neurons in the SSTKO mice. In the case of SSTR4, the small increase in the number of binding sites for this subtype was not detected by immunocytochemistry. Finally, the pattern of SSTR subtype expression at the protein level was paralleled by changes in SSTR mRNA levels. Because SSTR1 and 2 are the predominant subtypes in mouse brain, our results suggest that the net increase in membrane SSTRs in the SSTKO mouse is due largely to augmented expression of these two receptors. Our results are consistent with previous studies showing that chemical depletion of brain SST in the rat with cysteamine also up-regulates cortical membrane SST binding sites (30). In contrast, in human Alzheimer's disease, the loss of cortical SST is associated with a reduction in SST binding sites, suggesting that the neurodegenerative process targets both SST neurons and SST-receptive neural elements (4, 7). It will be interesting to determine whether there is an attempt at functional up-regulation of SSTRs in the early stages of Alzheimer's disease in response to falling cortical concentrations of SST. The finding that SSTRs are up-regulated in the absence of their natural ligand suggests that SST is capable of negatively regulating its own receptors, but whether this effect is direct or indirect is unclear. Like other GPCRs, SSTRs are acutely regulated at the membrane by agonist binding (3, 19, 31–33). Prolonged exposure of human SSTRs to agonist produces up-regulation of human (h) SSTR1 and, to a lesser extent, that of hSSTR2 and hSSTR4 (19, 20). These short- and long-term *in vitro* regulatory responses of SST on SSTR expression, however, fail to explain fully the pattern of SSTR subtype expression *in vivo* in the SSTKO mouse. For instance, SSTR3, which undergoes endocytosis in response to agonist activation, was also found to be down-regulated in the SST-deficient mouse (19). SSTR1, which is up-regulated by chronic agonist exposure, was also up-regulated *in vivo* in SST-deficient mice (20). In addition to these subtype-selective differences, there were tissue-specific variations in the pattern of expression of an individual subtype. For instance, SSTR1, which was generally up-regulated in most tissues, was differentially reduced in the hypothalamus and adrenals. Likewise, SSTR2, which was typically up-regulated in most tissues, was selectively down-regulated in the pituitary and adrenals, whereas SSTR3 was consistently decreased in both brain and peripheral tissues. Surprisingly, we could detect expression of SSTR1 mRNA only in the stomach, despite previously reported detection of mRNA for SSTR2 in rat stomach (28, 34) and the evidence from SSTR2 knockout mice suggesting that this receptor subtype may be involved in the regulation of gastric acid production (35). We can only speculate that perhaps the effects of SSTR2 removal on acid secretion are mediated via central SSTR2 receptors or via an indirect mechanism locally in the stomach.

Overall, this implies that the effect of SST deficiency on SSTR regulation *in vivo* is complex and because it is tissue specific, it is likely to be mediated indirectly rather than directly. In the case of other GPCRs, no consistent pattern of change in receptor expression has been found as a result of chronic deficiency of ligand. Mice deficient in dopamine do not show any change in expression of D1 and D2 receptors in the striatum (36). The GnRH-deficient mouse is characterized by a loss of pituitary GnRH receptors (37) whereas GHRH deficiency in rat hypothalamus leads to increased expression of pituitary GHRH receptors (38).

The pattern of expression of SST in mouse reported here is consistent with that described previously (2, 39). Deletion of the SST gene provided an opportunity for quantifying the concentration of CST relative to SST in brain, because previous estimates of the brain concentrations of SST-LI likely reflect a mixture of both SST and CST (40). Our results reveal that the brain content of CST is relatively low, constituting only approximately 5% of the total SST-/CST-like immunoreactivities. We found the highest level of CST mRNA expression in brain cortex in agreement with studies in rats and humans (22, 24). However, unlike the rat, CST expression in the mouse was also prominent in the hypothalamus, thalamus, and midbrain (21). Deletion of the SST gene did not augment CST mRNA expression in any brain region that normally expresses this gene, nor was there an induction of the CST gene in peripheral tissues. Rat and human prepro-CSTs are processed through endoproteolytic cleavage at dibasic sites, generating CST-14 and CST-29 in the rat, and hCST-17 and hCST-29 in humans (23). Mouse prepro-CST sequence contains only a single dibasic cleavage motif for a putative CST-14 product but lacks any recognizable cleavage motif for a CST-29 homolog (23). Consistent with the predicted processing pattern, HPLC analysis of CST-LI in brain extracts from SSTKO mice revealed a peak coeluting with synthetic CST-14 without a peak corresponding to synthetic CST-29. HPLC analysis, however, did reveal a second immunoreactive peak which eluted 4 min later than synthetic CST-29 (Fig. 8). The nature of this peak remains to be determined. It may be a mouse homolog of CST-29 that is derived through cleavage by enzymes different from the classical prohormone convertases, or it may represent the product of a different SST-related precursor.

Our finding of SST-like immunoreactivity in the pancreas and midgut of the SSTKO mice is of considerable interest. This material was present in small but readily detectable amounts in the pancreas and ileum and in high concentrations in the duodenum and jejunum. It was clearly not a product of the CST gene whose mRNA was undetectable in the intestine or any other peripheral tissue of the SSTKO mouse. By HPLC analysis, the immunoreactivity in the gut was resolved into a novel peak that eluted after the peak corresponding to pro-SST/pro-CST. Thus, by both mRNA and protein analysis, this material was not derived from the SST or CST genes. It appeared to be the product of a novel third SST-related gene that was

induced in the midgut in response to SST deficiency. The induction of auxiliary sources of hormone in response to specific hormonal deficits appears to be a common safety feature of endocrine regulation (41). Further studies to elucidate the structure of the intestinal SST-like gene are currently in progress.

SST has been implicated in the control of motor activity, in cognitive function, and in the modulation of sensory function (2, 39). Despite the increase in mRNA expression for SSTR2 and 5 in brain, the SSTKO mice displayed no overt behavioral abnormality. One explanation is that CST interacts with the up-regulated SSTRs to compensate for SST deficiency. Another more likely possibility is that SST deficiency does induce neuropsychological deficits, which, however, can only be detected by detailed behavioral testing. In this context, studies of neuroendocrine function in these mice have already shown an essential role of SST in the sexually diergic secretion of GH (25). Overall, our studies reveal that SST deficiency is compatible with life but produces a number of phenotypic changes. Further studies of central nervous system, metabolic, and immune cell function may reveal additional abnormalities that will help to define the full extent of the SSTKO phenotype and the essential biological functions of SST.

MATERIALS AND METHODS

Reagents

Synthetic peptides were obtained as follows: SST-14, SST-28 (Bachem, Torrance, CA); Tyrosinyl SST-14, Leu^{8}-D-Trp^{22}-Tyr^{25} SST-28 (LTT-SST-28), rat CST-14, and rat CST-29 (Peninsula Laboratories, Inc., Belmont, CA). Acetonitrile and trifluoroacetic acid were purchased from Fisher Scientific (Pittsburgh, PA). Heptafluorobutyric acid was obtained from Pierce Chemical Co. (Rockford, IL). All other reagents were of analytical grade and obtained from various manufacturers.

SST-Deficient Mice and Tissue Samples

SST-deficient mice were created by targeted disruption of the SST gene in embryonic stem cells followed by the derivation of transgenic *Smst*−/− mice as previously described (25). The mutated allele was backcrossed for five consecutive generations onto the C57BL/6J genetic background, and viable N5 homozygous offspring were produced in the normal Mendelian ratios from heterozygous breeding pairs. SSTKO and wt mice were sibling littermates derived from the mating of heterozygous breeder pairs. SST-deficient animals had normal gestation, birth and litter sizes and were viable and outwardly healthy. Adult mice of both genotypes were killed by decapitation. Whole brain, brain regions (frontal cortex, visual cortex, striatum, thalamus, hypothalamus, cerebellum) pituitary, stomach, pancreas, intestine, adrenal glands, liver, and gonads were removed by gross dissection, cleared from connective tissue and fat, and frozen immediately in liquid nitrogen. All procedures involving mice were approved by the Institutional Animal Care and Use Committee and conducted in accordance with accepted standards of humane animal care.

Binding Analysis

Membrane SSTRs were quantitated by binding analysis using [^{125}I]-LTT SST-28 radioligand, which binds to the five SSTR subtypes. Brain membranes were prepared as previously described (42). Whole brains were homogenized in 0.32 M sucrose, 20 mM Tris-HCl, 2.5 mM dithiothreitol (pH 7.5), with a glass homogenizer. The homogenate was centrifuged at 1000 rpm for 10 min. The supernatant was centrifuged at 10,000 rpm for 45 min and the pellet obtained was resuspended in the same buffer and centrifuged again at 12,000 rpm for 30 min. The final pellet was resuspended in 20 mM Tris-HCl buffer, an aliquot was removed for determination of protein content by the Bradford method, and the remaining sample was kept for membrane binding analysis. Saturation binding studies were carried out for 35 min at 37 C with 40 μg membrane protein and [^{125}I]-LTT SST-28 radioligand in 50 mM HEPES (pH 7.5), 2 mM $CaCl_2$, 5 mM $Mg\ Cl_2$, 0.5% BSA, 0.02% PMSF, and 0.02% Bacitracin (binding buffer), as previously described (20). Specific binding was defined as the difference in the amount of radioligand bound in the absence and presence of 100 nM SST-14. Saturation binding experiments were performed with membranes using increasing concentrations of [^{125}I]-LTT SST-28 under equilibrium binding conditions. To quantitate the concentration of individual SSTR subtypes, saturation binding analysis of whole-brain membranes was carried out with [^{125}I]-LTT SST-28 in the presence of a cocktail of nonpeptide agonists specific for each SSTR (43) but excluding the SSTR to be quantitated. The analogs L-797591 (SSTR1 specific) and L-779976 (SSTR2 specific) were used at 10^{-6} M; L-796778 (SSTR3 selective), L-803087 (SSTR4 selective), and L-817818 (SSTR5 selective) were used at 10^{-7} M. Incubations were terminated by the addition of 1 ml ice-cold binding buffer, rapid centrifugation, and washing. Radioactivity associated with membrane pellets was quantified in an LKB γ-counter (LKB-Wallach, Turku, Finland). Data analysis and calculation of kinetic constants was performed by Scatchard analysis with Prism 3.0 (GraphPad Software, Inc., San Diego, CA). Each experiment was repeated at least three times with samples from both wt and SSTKO mice analyzed in the same experiment. Membranes were prepared from different animals in several separate different extractions.

RIA of SST and CST

Immunoreactive SST (SST-LI) and CST (CST-LI) were both measured using a SST RIA that has been previously described in detail (40, 44). Brain and peripheral tissue samples from different animals were homogenized in 1 M acetic acid by sonication, boiled for 5 min, and aliquots were removed for protein estimation by the Bradford assay. The remaining extract was centrifuged at 8000 $\times$ *g* for 30 min, and the supernatant was neutralized and applied as samples in the RIA. RIA was performed using the rabbit anti-SST antibody (R149) directed against the central segment of SST-14, synthetic SST-14 standards, and a BSA-coated charcoal separation method. Antibody R149 recognizes both SST-14 and SST-28 equally and cross-reacts 72% with rat CST-14 and 68% with rat CST-29 (40).

HPLC

Mouse tissues from different animals were extracted in 1 M acetic acid by sonication, and extracts were analyzed by HPLC on a C18 μBondapak reverse phase column using a Waters HPLC apparatus (Waters Corp., Milford, MA) as previously described (45). The column was eluted at room temperature at 1 ml/min with a 12–55% acetonitrile and 0.2% heptafluorobutyric acid gradient over 150 min. The column effluent was monitored for UV absorbance at 214 and 280 nm. Fractions were collected in glass tubes, spiked with 10 μl

of 10% BSA, and aliquots (100–500 μl) were evaporated in a Speed-Vac and assayed for SST-14 LI (and/or CST LI) by RIA.

RT-PCR

mRNA for SSTR1-5 was analyzed by semiquantitative RT-PCR (18). Tissue samples were homogenized in Trizol reagent (Life Technologies, Inc., Gaithersburg, MD). Total RNA was isolated by the guanidinium isothiocyanate phenolchloroform extraction method. Samples were then incubated with RQ1 ribonuclease-free deoxyribonuclease (Promega Corp., Madison, WI) at 37 C for 30 min, and the deoxyribonuclease was inactivated and removed by phenol chloroform extraction. After precipitation of RNA by sodium acetate and ethanol, samples were redissolved in water, and the total amount of RNA was quantified by spectrophotometric measurement. The integrity of the RNA was confirmed by agarose gel electrophoresis and staining with ethidium bromide. For reverse transcription, 10 μg total DNA-free RNA were incubated in 40 μl reaction containing 20 mM Tris-HCl (pH 8.4), 50 mM KCl, 5 mM $MgCl_2$, 1 mM deoxynucleoside triphosphates, 8 U of RNasin (Promega Corp.), 100 pmol of random hexanucleotides (Pharmacia Biotech, Piscataway, NJ), and 400 U of Moloney murine leukemia virus reverse transcriptase (Life Technologies, Inc., Paisley, UK) at 42 C for 30 min. Four microliters of the resulting cDNA samples were denatured at 94 C in 20 mM Tris-HCl (pH 8.4), 50 mM KCl, 1.5 mM $MgCl_2$, (2 mM $MgCl_2$ and 5% dimethylsulfoxide for PCR of SST), 200 μM deoxynucleoside triphosphates, and 15 pmol each of SSTR1-5, SST, or CST primers in 100 μl reaction volume for 10 min. The primers used for SSTR1-5 were against the rat receptor sequences, as previously described, and were virtually identical with mouse SSTR sequences (18). The primers for mouse SST and CST have been previously published (25). The primers used for SSTR2 amplified only the SSTR2A isoform.

PCR was initiated by addition of 2.5 U of *Taq* polymerase (3 U for CST PCR) (Life Technologies, Inc.) at 85 C (hot start). The following conditions were used: SSTR1 and 2, denaturation at 94 C for 1 min, annealing at 52 C for 30 sec, and extension at 72 C for 90 sec; SSTR3, 4, and 5, denaturation at 94 C for 1 min, annealing at 54 C for 30 sec, and extension at 72 C for 90 sec; SST, denaturation at 94 C for 50 sec, annealing at 56 C for 35 sec, and extension at 72 C for 45 sec; CST, denaturation at 94 C for 1 min, annealing at 55 C for 45 sec, and extension at 72 C for 85 sec. SSTR1-5, SST, and CST were coamplified with β-actin for 27 cycles followed by final extension at 72 C for 10 min.

Southern Transfer and Hybridization

PCR products (30 μl) were separated by electrophoresis on 1.5% agarose gels, transferred to gene screen plus hybridization membranes (Bristol-Myers Squibb, Billerica, MA), and hybridized with ^{32}P-labeled SSTR1-5 and β-actin-specific cDNA probes. Probes were labeled to high specific activity by random hexanucleotide primers using a Life Technologies, Inc. Kit. After hybridization for 20–22 h at 65 C, filters were washed and exposed to Kodak X-AR film (Eastman Kodak Co., Rochester, NY) for various times. Autoradiograms were scanned in a Umax 610 P Scanner using the software Vista Scan 2.4 (Umax Data Systems, Inc., Pleasanton, CA). The hybridization signals were quantified with the Igor Pro 3.13 Analysis Software Package (Wave Metrics, Inc., Lake Oswego, OR). Total intensity of the blots (average optical density × area in pixels) was corrected for background and used as an index of SSTRs and actin mRNAs. Only bands that did not reach saturation density of x-ray film exposure were subjected to quantitative analysis. Values of SSTR1-5 mRNA expression were normalized to those of actin mRNA on the same gels. The same quantification method was used for analysis of SST and CST mRNA expression directly in ethidium bromide-stained gels of the corresponding PCR products. All experiments were performed three times, and each mRNA quantification represents an average of at least three measurements.

Immunohistochemistry

Brain sections from control and SSTKO mice were studied for expression of SSTR1-5 and SST/CST-LI by immunocytochemistry. Antipeptide rabbit polyclonal antibodies specific to SSTR1-5 and to SST were produced and characterized as previously described (16–18, 44). Mice were perfused with 4% paraformaldehyde in 0.1 M PBS, and the brain was removed and postfixed in 4% paraformaldehyde overnight. Free-floating vibratome sections (30–40 μm) were collected and treated with H_2O_2 1.5% and methanol 10% for 10 min to block endogenous peroxidase. Sections were then washed in PBS and incubated with 5% normal goat serum followed by incubation with primary antibodies to SSTR1-5 (diluted 1:200) or to SST (diluted 1:500) at 4 C for 24 h. After washing with Tris-buffered saline, sections were incubated with biotinylated goat antirabbit secondary antibody (diluted 1:200) at room temperature for 1.5 h, followed by exposure to avidin-biotinylated-peroxidase complex (Vectastain Elite, ABC Kit, Vector Laboratories, Inc., Burlingame, CA) in Tris-buffered saline for 1 h at room temperature. The reaction was revealed by chromogen 3.3′-diaminobenzidine, 0.5 mg/μl (Sigma, St. Louis, MO), containing 0.01% hydrogen peroxide yielding a brown-black reaction product. After three additional washes, sections were mounted and viewed under a microscope (Leica Corp., Deerfield, IL). Controls used to validate the specificity of the immunoreactivity included preimmune serum in place of primary antibody and primary antibody absorbed with excess antigen. The number of cortical neurons positive for SSTR expression in sections of control and SSTKO mice was analyzed quantitatively. Neurons immunopositive for SSTR1-5 were counted at low-power magnification (×10) in 11 fields and expressed as the number of immunopositive neurons/mm^2. A total of 1500–3200 neurons were analyzed for each receptor.

Statistical Analysis

Results are presented as mean ± SE. Statistical comparisons between genotypes were made by unpaired *t* test, comparing SSTKO samples with their correspondent wt values as paired data groups within the same experimental procedure. *P* values < 0.05 were considered statistically significant.

Acknowledgments

We thank M. Correia for secretarial help and L. Semaan for technical assistance. Subtype-selective nonpeptide SSTR agonists were obtained through the courtesy of S. P. Rohrer and J. M. Schaeffer (Merck Research Laboratories, Rahway, NJ). Y.C.P. is a Distinguished Scientist of the Canadian Medical Research Council.

Received February 8, 2002. Accepted March 27, 2002.

Address all correspondence and requests for reprints to: Dr. Y. C. Patel, Room M3-15, Royal Victoria Hospital, 687 Pine Avenue West, Montréal, Québec H3A 1A1, Canada. E-mail: yogesh.patel@mcgill.ca.

This work was supported by grants to Y.C.P. from the NIH (NS-32160) and the Canadian Institutes of Health Research (MT6196 and MT10411) and to M.J.L. from the Lucille P. Markey Charitable Trust and the Medical Research Foundation of Oregon. J.L.R. is a Fellow of the Fonds de

la Recherche en Sante du Québec (FRSQ) and Ministerio de Educacion y Cultura (MEC, Spain).

* Present address: Instituto de Investigaciones en Ingeniería Genética y Biología Molecular (CONICET) and Department of Biological Sciences, FCEyN, Universidad de Buenos Aires, Argentina.

REFERENCES

1. Reichlin S 1983 Somatostatin. N Engl J Med 309: 1495–1501, 1556–1563
2. Epelbaum J, Dournaud P, Fodor M, Viollet C 1994 The neurobiology of somatostatin. Crit Rev Neurobiol 8:25–44
3. Patel YC 1999 Somatostatin and its receptor family. Front Neuroendocrinol 20:157–198
4. Davies P, Katzman R, Terry RD 1980 Reduced somatostatin-like immunoreactivity in cerebral cortex from cases of Alzheimer's disease, and Alzheimer senile dementia. Nature 288:279–280
5. Martin JB, Guzella JF 1986 Huntington's disease: pathogenesis and management. N Engl J Med 315:1267–1276
6. Aronin N, Hooper PE, Lorenz LJ, Bird ED, Sagar SM, Leeman SE, Martin JB 1983 Somatostatin is increased in the basal ganglia in Huntington's disease. Ann Neurol 13:519–526
7. Beal MF, Mazurek MF, Tran VT, Chattha G, Bird ED, Martin, JB 1985 Reduced numbers of somatostatin receptors in the cerebral cortex in Alzheimer's disease. Science 229:289–291
8. Da Cunha A, Rausch DM, Eiden LE 1995 An early increase in somatostatin mRNA expression in the frontal cortex of Rhesus monkeys infected with simian immunodeficiency virus. Proc Natl Acad Sci USA 92: 1371–1375
9. Reisine T, Bell GI 1995 Molecular biology of somatostatin receptors. Endocr Rev 16:427–442
10. Breder CD, Yamada YY, Yasuda K, Seino S, Saper CB, Bell GI 1992 Differential expression of somatostatin receptor subtypes in brain. J Neurosci 12:3920–3934
11. Kong H, De Paoli AM, Breder CD, Yasuda K, Bell GI, Reisine T 1994 Differential expression of messenger RNAs for somatostatin receptor subtypes SSTR1, SSTR2, and SSTR3 in adult rat brain: analysis by RNA blotting and *in situ* hybridization histochemistry. Neuroscience 59:175–184
12. Meyerhof W, Wulfsen I, Schonrock C, Fehr S, Richter D 1992 Molecular cloning of a somatostatin-28 receptor and comparison of its expression pattern with that of a somatostatin-14 receptor in rat brain. Proc Natl Acad Sci USA 89:10267–10271
13. Thoss VS, Perez J, Duc D, Hoyer D 1995 Embryonic and postnatal mRNA distribution of five somatostatin receptor subtypes in the rat brain. Neuropharmacology 34: 1673–1688
14. Hervieu G, Emson PC 1998 The localization of somatostatin receptor 1 (sst1) immunoreactivity in the rat brain using an N-terminal specific antibody. Neuroscience 85: 1263–1284
15. Dournaud P, Gu YZ, Schonbrunn A, Mazella J, Tannenbaum GS, Beaudet A 1996 Localization of the somatostatin receptor SST2A in rat brain using a specific antipeptide antibody. J Neurosci 16:4468–4478
16. Kumar U, Laird D, Srikant CB, Escher E, Patel YC 1997 Expression of the five somatostatin receptor (SSTR1-5) subtypes in rat pituitary somatotrophes: quantitative analysis by double-immunofluorescence confocal microscopy. Endocrinology 138:4473–4476
17. Kumar U, Sasi R, Suresh S, Patel A, Thangaraju M, Metrakos P, Patel SC, Patel YC 1999 Subtype-selective expression of the five somatostatin receptors (hSSTR1-5) in human pancreatic islet cells: a quantitative double-label immunohistochemical analysis. Diabetes 48:77–85
18. Khare S, Kumar U, Sasi R, Puebla L, Calderon L, Lemstrom K, Hayry P, Patel YC 1999 Differential regulation of somatostatin receptor types 1–5 in rat aorta after angioplasty. FASEB J 13:387–394
19. Hukovic N, Panetta R, Kumar U, Patel YC 1996 Agonist-dependent regulation of cloned human somatostatin receptor types 1–5 (hSSTR1-5): subtype selective internalization or upregulation. Endocrinology 137:4046–4049
20. Hukovic N, Rocheville M, Kumar U, Sasi R, Khare S, Patel YC 1999 Agonist-dependent upregulation of human somatostatin receptor type 1 requires molecular signals in the cytoplasmic C-tail. J Biol Chem 274:24550–24558
21. De Lecea L, Criado JR, Prospero-Garcia O, Gautwik KM, Schwitzer P, Danielson PE, Dunlop CLM, Siggins GR, Henriksen SJ, Sutcliffe JG 1996 A cortical neuropeptide with neuronal depressant and sleep-modulating properties. Nature 381:242–245
22. De Lecea L, Del Rio JA, Criado JR, Alcantara S, Morales M, Danielson PE, Henriksen SJ, Soriano E, Sutcliff GJ 1997 Cortistatin is expressed in a distinct subset of cortical interneurons. J Neurosci 17:5868–5880
23. De Lecea L, Ruiz-Lozano P, Danielson PE, Peelle-Kirley J, Foye PE, Frankel WN, Sutcliffe JG 1997 Cloning, mRNA expression, and chromosomal mapping of mouse and human preprocortistatin. Genomics 42:499–506
24. Fukusumi S, Kitada C, Takekawa S, Kizawa H, Sakamoto J, Miyamoto M, Hinuma S, Kitano K, Fujino M 1997 Identification and characterization of a novel human cortistatin-like peptide. Biochem Biophys Res Commun 232:157–163
25. Low MJ, Otero Corchon V, Parlow AF, Ramirez JL, Kumar U, Patel YC, Rubinstein M 2001 Somatostatin is required for masculinization of growth hormone-regulated hepatic gene expression but not of somatic growth. J Clin Invest 107:1571–1580
26. Buckmaster PS, Otero-Corchon V, Rubinstein M, Low MJ 2002 Heightened seizure severity in somatostatin knockout mice. Epilepsy Res 48:43–56
27. Fehlmann D, Langenegger D, Schuepbach E, Siehler S, Feuerbach D, Hoyer D 2000 Distribution and characterisation of somatostatin receptor mRNA and binding sites in the brain and periphery. J Physiol Paris 94:265–281
28. Bruno JF, Xu Y, Song J, Berelowitz M 1993 Tissue distribution of somatostatin receptor subtype messenger ribonucleic acid in the rat. Endocrinology 133:2561–2567
29. Feuerbach D, Fehlmann D, Nunn C, Siehler S, Langenegger D, Bouhelal R, Seuwen K, Hoyer D 2000 Cloning, expression and pharmacological characterisation of the mouse somatostatin sst(5) receptor. Neuropharmacology 39:1451–1462
30. Srikant CB, Patel YC 1984 Cysteamine-induced depletion of brain somatostatin is associated with up-regulation of cerebrocortical somatostatin receptors. Endocrinology 115:990–995
31. Dohlman HG, Thorner J, Caron MG, Lefkowitz RJ 1991 Model systems for the study of seven transmembrane segment receptors. J Biol Chem 268:337–341
32. Hipkin RW, Friedman J, Clark RB, Eppler CM, Schonbrunn A 1997 Agonist-induced desensitization, internalization and phosphorylation of the sst2A somatostatin receptor. J Biol Chem 272:13869–13876
33. Roth A, Kreienkamp HJ, Nehrign RB, Roosterman D, Meyerhof W, Richter D 1997 Endocytosis of the rat somatostatin receptors—subtype discrimination, ligand specificity and delineation of carboxy-terminal positive and negative sequence motifs. DNA Cell Biol 16:111–119
34. Krempels K, Hunyady B, O'Carrol AM, Mezey E 1997 Distribution of somatostatin receptor messenger RNAs in

the rat gastrointestinal tract. Gastroenterology 112: 1948–1960
35. Martinez V, Curi AP, Torkian B, Schaeffer JM, Wilkinson HA, Walsh JH, Tache Y 1998 High basal gastric acid secretion in somatostatin receptor subtype 2 knockout mice. Gastroenterology 114:1125–1132
36. Zhou Q-Y, Palmiter RD 1995 Dopamine-deficient mice are severely hypoactive, adipsic, and aphagic. Cell 83: 1197–1209
37. Young LS, Detta A, Clayton RN, Jones A, Charleton HM 1985 Pituitary and gonadal function in hypogonadotrophic hypogonadal (hpg) mice bearing hypothalamic implants. J Reprod Fertil 74:247–255
38. Kovacs M, Kineman RD, Schally AV, Flerko B, Frohman LA 2000 Increase in mRNA concentrations of pituitary receptors for growth hormone-releasing hormone and growth hormone secretagog after neonatal monosodium glutamate treatment. J Neuroendocrinol 12:335–341
39. Patel YC 1992 General aspects of the biology and function of somatostatin. In: Weil C, Muller EE, Thorner MO, eds. Basic and clinical aspects of neuroscience. Berlin: Springer-Verlag; vol 4:1–16
40. Puebla L, Mouchantaf R, Sasi R, Khare S, Bennett HPJ, James S, Patel YC 1999 Processing of rat preprocortistatin in mouse AtT-20 cells. J Neurochem 73:1273–1277
41. Gunther T, Chen Z-F, Kim J, Priemel M, Rueger JM, Amling M, Moseley JM, Martin TJ, Anderson DJ, Karsenty G 2000 Genetic ablation of parathyroid gland reveals another source of parathyroid hormone. Nature 406:199–203
42. Srikant CB, Patel YC 1981 Somatostatin receptors: identification and characterization in rat brain membranes. Proc Natl Acad Sci USA 78:3930–3934
43. Rohrer SP, Birzin ET, Mosley RT, Berk SC, Hutchings SM, Shen DM, Xiong Y, Hayes EC, Parmar RM, Foor F, Mitra SW, Degrado SJ, Shu M, Klopp JM, Cai SJ, Blake A, Chan WWS, Pasternak A, Yang L, Patchett AA, Smith RG, Chapman KT, Schaeffer JM 1998 Rapid identification of subtype-selective agonists of the somatostatin receptor through combinatorial chemistry. Science 282: 737–740
44. Patel YC, Reichlin S 1978 Somatostatin in hypothalamus, extrahpothalamic brain and peripheral tissues of the rat. Endocrinology 102:523–530
45. Galanopoulou AS, Kent G, Rabbani SN, Seidah NG, Patel YC 1993 Heterologous processing of prosomatostatin in constitutive and regulated secretory pathways: putative role of the endoproteases furin, PC1, and PC2. J Biol Chem 268:6041–6049